The role of algae in fine sediment flocculation: In-situ and laboratory measurements

Deng, Zhirui; He, Qing; Safar, Zeinab; Chassagne, Claire

DOI
10.1016/j.margeo.2019.02.003

Publication date
2019

Document Version
Accepted author manuscript

Published in
Marine Geology

Citation (APA)
Deng, Z., He, Q., Safar, Z., & Chassagne, C. (2019). The role of algae in fine sediment flocculation: In-situ and laboratory measurements. *Marine Geology*, *413*, 71-84. https://doi.org/10.1016/j.margeo.2019.02.003

The role of algae in fine sediment flocculation: in-situ and laboratory measurements

Zhirui Deng[a], Qing He[a, *], Zeinab Safar[b], Claire Chassagne[b]

[a] State Key Laboratory of Estuarine and Coastal Research, East China Normal University, Shanghai 200062, People's Republic of China

[b] Section of Environmental Fluid Mechanics, Faculty of Civil Engineering and Geosciences, Delft University of Technology, PO Box 5048, 2600, GA, Delft, The Netherlands

[*] Corresponding author.

E-mail address: qinghe@sklec.ecnu.edu.cn (Q. He).

Abstract

The precise interactions between organic and inorganic particles in the context of flocculation is an on-going topic of research. The suspended particulate matter (SPM) found in estuaries is composed of both organic and inorganic particles with specific particle size distributions (PSD's). These PSD's are a function of the hydrodynamic conditions, suspended sediment concentration (SSC), organic matter composition, salinity and seasonal variations. A field campaign was carried out in August 2015 in the turbidity maximum zone of the Yangtze Estuary, where the SPM dynamics were recorded. The concentration of algae in the water column was indirectly measured through the chlorophyll-a concentration (CC). We show that there is a strong correlation between SSC and CC in the whole water column, for the whole tidal cycle. Additional flocculation experiments in the laboratory confirm that the largest observed flocs are predominantly organic-based, and that salinity alone could not induce the flocculation of the Yangtze mineral particles. A key parameter for the

maximal floc size is the algae concentration to sediment concentration ratio. When this ratio is high, the D50 is high and vice-versa.

Key words: Flocculation; Algae; Yangtze Estuary; Grain size distribution; Floc size; Tidal variation

1. Introduction

Transport of fine-grained sediment in estuarine areas is a highly dynamic process, and is primarily controlled by river discharge, tidal energy and wave action as well as suspended matter load in the estuarine water. Flocculation and break-up are important processes of estuarine sediment transport as they govern the floc size, shape, strength, density, which in turn modifies the sediment settling velocity. The settling velocity is a main parameter for sediment transport and deposition models.

A lot of work has been done to study the physical flocculation/break-up mechanisms in estuaries (Cheng, 2004; Fennessy and Dyer, 1996; Mietta, 2010; Verney et al., 2009). The influence of shear stresses and sample composition (clay type, chemistry) has been investigated, both in-situ and in the laboratory (Manning, 2010; Manning and Dyer, 1999; Mietta, 2010; Mikkelsen and Pejrup, 2001; Winterwerp, 1999). More recently, the influence of microorganisms such as phytoplankton on sediment flocculation have been investigated (de Lucas Pardo, 2014; Fettweis and Lee, 2017; Huiming et al., 2011; Kiørboe et al., 1994; Lee, 2000a; Maggi, 2009, 2013).

The present research was motivated by the following observation: we found, after analyzing the results of our field campaign in the Yangtze Estuary, that most of the recorded particle size distributions were bimodal, with a small size peak around 20 μm and a large particle peak around

200 µm. Standard flocculation models, based on the population balance equation (Mietta et al., 2010; Nopens, 2005;; Winterwerp, 2002, 1998) do not account for bimodal distributions. Recently, quite some work has been initiated on population balance equations accounting for both physical and bio-chemical effects (Verney et al., 2011; Shen et al., 2018; Lee et al., 2012, 2011). All these models require several input parameters, in particular the collision efficiency and frequency, a break-up function and the number of microflocs (or primary particles) inside a macrofloc. Multimodal distributions can be achieved:

Hypothesis 1 - at steady-state for two types of particles (organic and inorganic for example), each type having different aggregation and break-up mechanisms and not significantly interfering with each other. This can happen for example in sediment-rich environments where organic-based flocs cannot "take-up" sediment anymore. Both mineral flocs and organic-based flocs have then their own aggregation/break-up mechanisms under shear.

Hypothesis 2 - by considering a same floc population having different modes of break-ups (binary/ternary), and/or accounting for floc erosion (Verney et al., 2011).

Hypothesis 3 – by having Population Size Distributions (PSD's) not yet at steady-state. An inflow of sediment particles in a water column containing organic matter for example can also be multimodal. If the aggregation between sediment and organic matter is optimal a monomodal distribution could be achieved at steady-state.

From in-situ data, it is difficult to distinguish which of the mechanisms is responsible for the observed multimodal distribution. Hypothesis 1 and 3 were tested in laboratory studies on sediment and algae where we could study PSD's reaching steady-state.

Based on the results of past research, it is known that algae, and in particular diatoms, combined

with sediment, produce large aggregates (Droppo, 2001; Fettweis and Lee, 2017; Passow et al., 1994). Diatoms are a common type of phytoplankton and are found in the whole water column in estuaries. Their concentration varies with the seasons and is highest usually in spring and summer in the Yangtse estuary (Zhu et al., 2009). . These algae always coexist with sediment particles in estuaries. The relationship between algae and flocculation has been established for a long time. In the early 1960's, the aggregation of suspended particles with Anabaenopsis and their excreted substances has been studied (Walsby, 1968). The earliest SEM picture of a floc composed of the algae Cyanophyta with sediment has been published in 1982 (Avnimelech et al., 1982). This study also showed that the presence of Cyanophyta enhanced the flocculation ability of the sediment. Kiørboe et al. (Kiørboe et al., 1994, 1990) noticed from in-situ observations in the Danish Ise Fjord that sediment could aggregate with diatoms. As each algae species has different shape, size and surface properties, the flocculation involving one algae type or another create different flocs. For example, De Lucas Pardo et al. (de Lucas Pardo, 2014) investigated the flocculation involving two algae species (*Aphanizomenon* and *Aphanothece*). In the presence of clay particles and *Aphanizomenon*, filamentous small flocs were produced, whereas large isotropic flocs where produced in presence of *Aphanothece* and clay.

An important component in flocculation by algae is Extracellular Polymeric Substance (EPS) that is generated by the algae. This EPS is composed for a large part of polysaccharides (anionic or cationic carbohydrates) (Plude et al., 1991). EPS plays a significant role as flocculating agent as EPS can bind onto anionic sediment particles by cationic bridging (Dontsova and Bigham, 2005). The flocculation by different algae species and EPS sorts is an on-going topic of research. In order to improve the input parameters for flocculation models, a better understanding of the

sediment/algae interaction is required (Chen et al., 2005; Fettweis et al., 2014; Maggi, 2009) In the present article, in view of the parametrisation of our flocculation model, we answer the specific following questions, from in-situ measurements, for the Yangtse estuarine system:

1 – How is the Particle Size Distribution (PSD) evolving as function of depth and time?

2 – What is the corresponding sediment/algae ratio?

From complementary laboratory measurements, we investigate the following questions:

3 – Can sediment particles aggregate without the presence of algae?

4 – Can algae particles aggregate without the presence of sediment?

5 – What is the evolution of the PSD as function of time, when sediment and algae are put in presence? Are the found PSD representative for the ones found in-situ?

2. Methods

A field survey was carried out with state-of-the-art instruments and covered a whole tidal cycle in the Yangtze estuary. For the in-situ data, the vertical distribution in a tidal period of flocs are given. Chlorophyll-a is used as a proxy for determining the presence of algae., (Knap et al., 1996). The flocculation mechanisms between sediment and algae were investigated more into detail in the laboratory with the help of microscopy and static light scattering techniques. Although the domination of *Skeletonema costatum* tend to decrase in recent years, *Skeletonema costatum* are generally considered to be the most important population in the Yangtze estuary (Jiang et al., 2014). So this most common diatom (*Skeletonema costatum*) was used for the laboratory studies.

2.1 Study site

A whole tidal cycle sampling program was carried out from 14th to 22nd of August 2015 on a ship in the South passage of Yangtze Estuary.In this article, we analysed two successive tidal cycles: spring tide (08-14 to 08-15) and neap tide (08-20 to 08-21) . Each period included 26 hours of continuous observation. The wind condition was about 1–6 $m \cdot s^{-1}$ and stable. The morphology of the Yangtze Estuary shows bifurcations into four outlets. These are referred to as the North Branch, North Channel, North Passage, and South Passage (Figure 1). During the observation, the river discharge of Yangtze river was about 21,900–31,000 $m^3 \cdot s^{-1}$. In recent decades, the sediment load from Yangtze river decreased significantly compared to early decades (1950–2003) from an average of 4.22×10^9 $t \cdot yr^{-1}$ to an average of about 1.43×10^9 $t \cdot yr^{-1}$ in 2003–2011. The sediment load is estimated to be about 2.62×10^7 t in August 2015.

In the South Passage, the average tidal range is about 2.6 m. in this case, the spring tidal water depth ranges from 5 to 9 m and neap tidal depth ranges from 5.3 to 8.3 m. Tidal current can reach up to 1 $m \cdot s^{-1}$ in surface water (Chen, 1995). The study site (31°03′N, 122°04′E) is close to the salinity front, located at the surface at 123ºE, running from northwest to southeast. The intrusion of 31‰ continental shelf water can reach 122º20′E. The concentration of chlorophyll-a (which is a proxy for algae concentration) in the South passage has been given in (Chen, 1999), see their fig.5, and shows a spatial variation, with values ranging from 5 to 30 $mg \cdot m^{-3}$ (= 5 to 30 $\mu g \cdot l^{-1}$). In the surface water ,the average chlorophyll-a concentrations from 1998 to 2010 is 3 to 7 $\mu g \cdot l^{-1}$ near the study site, being high in late spring and summer while low in winter.The river discharge is a key parameter influencing the chlorophyll-a concentration (and hence the algae concentration) as it is a source of nutrients (Wang et al., 2015). The suspended sediments in the Yangtze Estuary are mostly

fine-grained particles. 60%–70 % of surface layer sediments are consist of silt (3.9–62.5 μm). The D_{50} of the dispersed suspended sediment is 7–11 μm, whereas the median size range of the bottom sediment is 15–300 μm (although there are spatial variations) (Liu et al., 2007). The Suspended Sediment Concentration (SSC) in the Yangtze Estuary varies greatly over time and space, ranging from 0.1 to 20 $g \cdot l^{-1}$.

2.2 Data collection

Flocs–and especially large ones–are so fragile in nature that in-situ monitoring is necessary (Chen and Eisma, 1995; Manning and Dyer, 1999). The floc parameters were recorded by LISST-100X with the path length reduction module (PRM) of 90%. The LISST-100X is a submersible multi-parameter system for in-situ measurements. A particle size distribution and volume concentration is obtained by small-angle light scattering (670 nm diode laser). The silicon detector has 32 specific log-spaced angle ranges. The raw data is post-processed to obtain sediment size distribution and volume. The validity of the data was assessed by checking the transmission value (in the original data) which should be between 0.3 to 0.9 (Pottsmith, 2015) .

The OBS-3A (Optical Backscatter Sensor) is an optical sensor that measures turbidity. Temperature was also recorded. The amount of chlorophyll-a found in a water sample was used to estimate the concentration of phytoplankton (algae) and was recorded with a Manta2 instrument (Water Quality Multiprobe, Eureka Environmental Engineering Company).

The fluorescence sensors were used to induce chlorophyll-a fluorescence by shining a beam of light of corresponding wavelength (435-470 nm) into the water and then measuring the higher wavelength light which was emitted (Pottsmith, 2015). All the instruments were attached together

to make sure that all the detectors would measure at the same position. All the instruments were set to record at an interval of 1 second. A full vertical profile was measured every hour and the instruments were pulled slowly from bottom to surface at the speed of 0.05 $m \cdot s^{-1}$. At specific locations in the water column, corresponding to the positions where the water samples are taken (see underneath), the instruments were left for 2 min at the same position in order to acquire statistically significant data. The data presented in the article is the average over the 2 min period. The hydrodynamic parameters were measured by ADCP (Acoustic Doppler Current Profiler, 300 kHz), which was set up 0.5 m under the ship with a 1.71 m blanking distance and a vertical resolution (bin size) of 0.5 m. Records of the water current direction and velocity were done in real time.

In addition, water samples were collected for calibration by 1.2L water sampler (horizontal trap sampler), then divided into two glass bottles, one for SSC analysis and another for Chl analysis. We took these double water samples at 6 vertical heights (0H, 0.2H, 0.4H, 0.6H, 0.8H, 1H) per hour In our definition, 0H represents the surface and 1H the bottom. The height corresponding to 1H was sampled at 0.5 m above the bed. A water sample for each height was filtered through a 0.45 μm cellulose acetate pre-weight filter paper, dried and weighted to estimate the sediment concentration distribution through the water column. The other water sample was filtered through a 0.45 μm ultra-fine glass fiber filter paper and stored at -20 ℃ for chlorophyll-a measurements in laboratory. The chlorophyll-a concentrations are for neap tide only as no water samples were taken at spring for chlorophyll-a analysis.

The chlorophyll-a concentration can be calculated as follows (Knap et al., 1996):

$$\mathrm{Chl} = (\mathrm{F_b} - \mathrm{F_a} - \mathrm{Blk_b} + \mathrm{Blk_a})\frac{\tau}{\tau - 1}\mathrm{F_R}\frac{\mathrm{V_{EXT}}}{\mathrm{V_{FILT}}} \quad (1)$$

Where F_b is the fluorometric reading of sample with 90% acetone, F_a is the fluorometric

reading of sample with 90% acetone and 10 % HCl. Blk_b is the fluorometric reading of pure 90% acetone, Blk_a is the fluorometric reading of pure 90% acetone with 10 % HCl. Linear calibration factors (F_R) are calculated as the slopes of the unacidified fluorometric readings vs. chlorophyll-a concentrations calculated spectrophotometrically. The acidification coefficient (τ) is calculated by averaging the ratio of the unacidified and acidified readings ($\tau = (F_b - Blk_b)/(F_a - Blk_a)$) of pure chlorophyll-a. V_{EXT} is the extraction volume by acetone extraction method and V_{FILT} is the filtrate volume of the water sample.

2.3 Shear stress estimation

To estimate the shear stress in the water column, the velocity data should be converted into shear rate G (Guo et al., 2017; Pejrup and Mikkelsen, 2010):

$$\mathrm{G}(z, H, u_*) = \sqrt{\frac{u_*^3 \times (1 - z/H)}{\nu \kappa z}} \quad (2)$$

Where ν is the kinematic viscosity of the water [$m^2 \cdot s^{-1}$], H is the total water depth [m], z is the height above bed, κ is Von Karman's constant (assumed to be 0.4) (Chien and Wan, 1999). The friction velocity, u_* [$m \cdot s^{-1}$] is given by:

$$u_* = \frac{u(z) \times \kappa}{\ln\left(\frac{z}{z_0}\right)} \quad (3)$$

Where $u(z)$ is the current velocity amplitude [$m \cdot s^{-1}$] at one of the 6 cells, where $z = xH$ and $x = 0.2, \ldots, 1$. The cell corresponding to $z = 1H$ was always sampled 0.5 m above the bed. z_0 is assumed to be constant and equal to 3 mm in accordance with the work of Guo et al. who investigated the same system in the same conditions (Guo et al., 2017).

The Kolmogorov micro-scale λ_0 is usually considered as the limits of floc size, which is the

smallest dissipating eddies length (van Leussen, 1999). It can be estimated by:

$$\lambda_0 = (\nu^3/\varepsilon)^{1/4} \quad (4)$$

Where ε is the turbulent energy dissipation ($m^2 \cdot s^{-3}$) which is linked to G given above by $G = \sqrt{\varepsilon/\nu}$ (Camp, 1943).

2.4 Laboratory experiments

Yangtze sediment grab samples, taken at the in-situ observation station, were used for the laboratory experiments in the Netherlands. As *Skeletonema costatum* represents over 90% of the algae species in Yangtze Estuary (He and Sun, 2009) this species was used in the laboratory tests. The algae was bought from Roem van Yerseke B.V. (The Netherlands) and used within a few days following the purchase.

Static Light Scattering

The static light scattering (SLS) experiments were performed using a Malvern Mastersizer (Mietta, 2010). The principles of the LISST and the Malvern MasterSizer are quite similar (Filippa et al., 2011). From the SLS measurements a full particle size distribution (size range 2nm–2mm in 100 log-spaced bins) was recorded every 30 s, enabling to follow flocculation in time. Sediment and algae sample were added to a mixing jar, and stirred by a paddle at the lowest speed possible to keep particles suspended.The samples were pumped into instrument and back to mixing jar continuously through two pipes of diameter 6 mm. The mixing jar was 0.125 m wide and 0.185 m high. There are significant differences between the turbulent mixing in the laboratory and in-situ. The shear rates in the jar/pump system are estimated from

$$G = 4Q/\pi r^3 \quad (5)$$

where Q is the discharge ($m^3 \cdot s^{-1}$) and r is the radius of the pipe (3 mm). Using a minimum shear

rate of about 90 s^{-1}, the Kolmogorov micro-scale λ_0 is about 110 µm. This shear rate is higher than the one created on average in the jar (Mietta, 2010) and is therefore the one we will consider here as limiting factor for aggregation. As the mean particle sizes found in-situ are lower than 100 µm using larger shear rates in the laboratory than in-situ should not affect significantly the comparisons between mean particle sizes in-situ and in the laboratory. It has been shown that the shear rate distribution in the jar affect the shape of the floc size distribution but not the mean floc size (Bouyer et al., 2004).

Another difference is the residence time in the jar: as the particles are kept in suspension, their collision probability and frequency will be higher than in-situ.

Microscopy

The pictures of (flocculated) algae were taken using a Digital Microscope (VHX 5000 Series). Flocs were sampled from the mixing jar, put onto a clean glass slide covered by another glass slide and visualized.The required confinement of the flocs between two glass slides affects the structure of the flocs and therefore the recorded sizes of flocs were smaller than the ones measured in-situ.

3. Results

3.1 In-situ versus laboratory OBS and chlorophyll-a estimations

The OBS response of clay particles of 2 µm is 50 times larger than the response of sand particles of 100 µm for the same concentration (Sutherland et al., 2000). Hence, each sensor was calibrated using sediment from the site of interest. The calibration was done using filtration results performed on in-situ water samples, see Figure 2 . In-situ measurements of chlorophyll-a were validated through laboratory (extraction) methods. The validation is also shown in Figure 2 .

The slope found for the sediment concentration measured in the laboratory versus the turbidity found in-situ is similar in spring and neap, indicating that the particle size distributions are not extremely different between these tides (Baker et al., 2001; Baker and Lavelle, 1984). The relation between the chlorophyll-a concentrations measured in-situ and in the laboratory is fairly linear, with an average slope of 0.90, but with an offset at origin: when chlorophyll-a is found to be 0 $\mu g \cdot l^{-1}$ in the laboratory, it has a value of 2 $\mu g \cdot l^{-1}$ in-situ. The chlorophyll-a concentrations (CC) presented in the article were corrected using the laboratory calibration.

3.2 Hydrodynamics, and salinity

The depth average current velocity and shear stress distribution and salinity gradients are shown in Figure 3. Due to tidal asymmetry, the maximum current velocity appears at ebb tide, and can be up to 1.5 $m \cdot s^{-1}$ at spring tide. At slack water, the current velocity is about 0.4 $m \cdot s^{-1}$ on average in the water column. The shear rate at the bottom of the water column is larger than that at the surface of the water column, and can reach 50 s^{-1}. The velocity and shear rate at spring tide are larger than at neap tide, but their distribution in the water column is similar.

At spring tide, salt sea water moves upstream and the salinity varies from 5 to 20 PSU. At neap tide, the salinity decreases and varies between 6 and 15 PSU. A low salinity surface plume is observed at ebb for spring tide. This is caused by the constant fresh water discharge which is spread out by the tidal current. The salinity is uniform during the flood period, being as large as 20 PSU, due to strong convection currents which are caused by oppositely directed river discharge and tidal current. At neap tide the salinity is uniformly distributed over the water column and remains on average below 12 PSU.

3.3 Suspended sediment, floc and chlorophyll-a characteristics

Distribution of sediment concentration and floc size and chlorophyll-a concentration are shown in Figure 3. The grey zones in the bottom figures indicate that no reliable LISST data could be obtained, due to the high SSC values.

The distribution of suspended sediment concentration (SSC) and chlorophyll-a concentration (CC) are clearly correlated. A more detailed description of the correlation will be given in section 4.2. Their distributions change with the tidal cycle. High SSC and CC concentrations appear at high shear stress, and their concentrations at the surface are lower than that at the bottom of the water column. The SSC was lower than 1 g·l-1 in the upper half of the water column for both spring and neap tides. At spring/neap tide the SSC reached values between 1-3 $g \cdot l^{-1}$ / 0.5-2 $g \cdot l^{-1}$ for the lower half of the water column at maximum flood velocity.We note that even though the total sediment concentration (which varies from 0 to 7 $g \cdot l^{-1}$) at spring tide is much higher than at neap tide (where it varies from 0 to 2 $g \cdot l^{-1}$), the chlorophyll-a concentration is similar between spring tide and neap tide, being no more than 7 $\mu g \cdot l^{-1}$.

The mean floc size (D_{50}) ranges from 20 μm (high shear stress) to 120 μm (low shear stress) with an average of 60 μm. Large flocs of about 60 to 80 μm are found at low shear rate conditions at slack water periods, for both high and low salinity conditions, at neap and spring tides. These flocs are distributed over the whole water column. At high water velocity, even though the largest SSC are then found, no large flocs are then observed in the upper half of the water column. The floc size could not be recorded in the lower part of the water column due to the high turbidity (Andrews et al., 2010).

4 Discussions

In a natural environment, flocculation can be affected by many factors, such as shear stress, salinity, presence of organic matter, etc.… (van Leussen, 1994). The change in salinity is not likely to be one of these factors, as the overall salinity is too high to be responsible for a significant change in flocculation. Indeed, the overall salinity is about 5–20 PSU whereas salt-induced flocculation is promoted in the transition range between 0 PSU and 3 PSU (Chassagne et al., 2009; Guan et al., 1996; Guan and Chen, 1995). The temperature is neither a factor, as the changes in temperatures are very small (the temperature varies between 25–30°C for all recording, not shown). In this section, we will distinguish between the evolution of the mean floc size D50 and its density as function of shear (subsection 4.1), the evolution of the full Particle Size Distribution PSD (subsection 4.2) and the role of algae (subsection 4.3). We will in particular show in 4.3 that the ratio CC/SSC (ChlorophyllA concentration divided by suspended sediment concentration) is an interesting proxy.

4.1 Shear rate influence on the mean floc size (D50) and its density

Shear stress is usually the main factor influencing the size and density of flocs in a dynamic environment (Eisma, 1986; Manning and Dyer, 1999; Winterwerp, 2002). Figure 4 shows the relationship between floc size and density with shear rate. As expected, the mean floc size decreases with increasing shear rate (fig.4a). This is true for all shear rates, even the lowest ones, indicating that (1) the flocs are either breaking or restructuring to flocs of higher density and smaller size when the shear rate is increasing and/or (2) denser (mineral) particles are flowing in the water column or are resuspended from the bed. This is in line with the results found for the density as function of shear rate, see Fig.4b. The density $\Delta\rho$ was calculated from the LISST and OBS data, using

equation (6)(Fettweis, 2008; Verney et al., 2009):

$$\Delta\rho = \rho_F - \rho_W = \left(1 - \frac{\rho_W}{\rho_P}\right)\frac{M_P}{V_F} \quad (6)$$

Where ρ_F is the floc density, ρ_W is the water density, ρ_P is the sediment particle density which is estimated to 2650 g·l^{-1}, M_P is the mass suspended sediment concentration obtained from the OBS and V_F is the floc volume concentration from LISST.

At spring tide, the floc effective density is increasing from below 200 g·l^{-1} for the lowest shear rates (< 5 s^{-1}) to > 300 g·l^{-1} for shear rates above 10 s-1 indicating that denser particles are in suspension at high shears. At neap tide, there is no correlation between effective density and shear rate, and the effective density remains low (below 200 g·l^{-1}) for all shears, implying that mainly organic-rich particles are in suspension. From Figure 4c, it is observed that the smallest particles have the highest effective density, for all depths and shear rates, and that there is no correlation between D50 and depth. In the next subsection, we will see that correlations can nonetheless be found as function of depth and shear rates when the full Particle Size Distribution (PSD) is studied.

4.2 Evolution of the Particle Size Distribution at different hydrodynamic conditions Figure 5 shows the full particle size distribution (PSD) in the water column, for different periods (termed MFV, HWS, MEV, LWS, see below). Both spring and neap periods display the same features. Several types of PSD's can be observed.

Three classes of particles of particles are distinguished: (1) particles smaller than 5 μm (2) particles in the range 10-50 μm and (3) particles in the range larger than 100 μm.

4.2.1 At Maximum Flood Velocity (MFV) and Maximum Ebb Velocity (MEV)

At MFV and MEV, The PSD is rather similar at all positions in the whole water column.

The small particles (< 5 μm) are particularly abundant at all maximum velocities (MFV, MEV) and are a function of shear rate. Their concentration increases with depth, where the highest shear rates are found (see Figure 2). There are more of these small particles at spring than at neap tide, as the shear rates are higher at spring compared to neap tides. These particles also have a high density (see Figure 4c) and as they are found primarily close to the bed it would tend to prove that they are mineral sediment particles resuspended from the bed.

The particles of size 10-50 μm and >100 μm are found over the whole water column in almost same proportion, except at the surface (0H, 0.2H) where there appears to be more >100 μm particles. These large particles (> 100 μm) are most probably algae, as their density should be low.

At MFV and MEV, the particles in the size range 10-50 μm are dominant in volume % compared to the other sizes, implying that the D50 will be in reasonably good approximation representative of that size fraction range, as can be seen in Table 1. From Table 1, it can however be noticed that the D50 is slightly biased by the presence of the largest particles from the range >100 μm, as the D50 at spring-MEV (where these large particles are significantly present, especially at the top of the water column) is larger than the D50 at spring-MFV, even though the peak in the size range 10-50 μm is not varying. The same occurs for the D50 at neap-MFV (where the large particles are present) which it is larger than the D50 at neap-MEV, but in this case there is also a shift in the 10-50 μm peak towards higher sizes for the particles at the bottom of the water column. This implies that at neap, the shear stresses are low enough to induce a particle size stratification in the water column.

At maximum velocity, with the D50 being in the range 15-25 μm, it can be observed from fig.4c that these particles have a wide spreading of density. This is the consequence of the fact that

the suspended particles are a mixture of dense small particles (of size < 5 μm), large particles with low density (of size > 100 μm), and a significant amount of particles in the 10-50 μm range, with variable density.

4.2.2 At High Water Slack (HWS) and Low Water Slack (LWS)

At HWS and LWS, the particles in the size range 10-50 μm are not always dominant in volume % compared to the size range >100 μm. . For instance, at Spring-LWS, a significant amount of particles are observed at the top of the water column (0H-0.2H) with a peak in size centered at about 20 μm and a large amount of particles with a peak in size centered at about 200 μm is observed at the bottom (0.8H–1H). There is a transition between the relative ratio of the two peaks (small / large particles) occurring between 0.4H and 0.6H, where the magnitude of the two peaks is the same. A similar trend is observed at neap, both for HWS and LWS.

At slack water, the shear stresses are low, and there is a shift of the D50 towards higher sizes compared to the maximum velocity case (see Table 1 and Figure 4a) . The particles observed at slack must have therefore an effective density that is low enough to keep them in suspension. It can in particular be observed that large particles (> 100 μm) are present at all depths at slack. This leads us to conclude that these particles are most probably algae and algae-rich particles.

There remains also a small background concentration of particles < 5 μm at all depths. These particles, whatever their density, remain primarily in suspension because their gravity-driven settling velocity is very low (their mass is very low).

At slack, with the D50 being in the range 45-55 μm, it can be observed from fig.4c that these particles have a narrow spreading in density, and that their density is very low. This is the

consequence of the fact that the particles in suspension are predominantly algae and algae-rich particles.

4.2 Role of algae in the particle size distribution

We have found (see section 4.1) that the full PSD in the water column is tri- or bimodal, depending on the hydrodynamic conditions. We have identified the smallest class size (< 5 μm) as being primarily composed of dense mineral sediment particles eroded from the bed and the largest class size (> 100 μm) as being primarily composed of algae with a low density. It remains to be investigated what the middle size class 10-50 μm is composed of. This raises the question whether and how mineral sediment interact with algae.

From fig.5 we have seen that the PSD is primarily multimodal. As stated in the introduction, a multimodal PSD can be due to several reasons. The smallest and the largest size classes (< 5 μm and > 100 μm) are present for all hydrodynamic conditions. This could imply that these particles do not interact significantly (hypothesis 1) with the middle class size 10-50 μm, or that the PSD is has not reached a steady-state due to the changing hydrodynamic conditions or the new inflow of particles (hypothesis 3).

Hypothesis 2 was based on the fact that a same floc population could have different modes of break-ups (binary/ternary), however we discard this hypothesis in our case. Indeed, if only one type of particles would be present, one would expect that for similar shears, there would be a correlation between sediment concentration (SSC) and floc size, as the collision frequency increases with SSC (Eisma and Li, 1993; Law et al., 2013; Lee, 2000b). The correlation between D50 and SSC is not good, see Figure 6, and one can even argue that there is a small trend indicating that the D50

decreases with SSC . This trend has also been found by other authors (Manning and Schoellhamer, 2013). This led us to conclude that the particles in the middle class size 10-50 μm (which is strongly correlated to the behaviour of the D50, as detailed in section 4.1) are composed of two types of particles: sediment and algae.

As can be seen in Figure 3, the chlorophyll-a concentration and SSC are strongly correlated. This correlation is better visible in Figure 7.

It is long known that sedimentation is a main cause for the distribution of phytoplankton in the water column (Barlow, 1955). Phytoplankton particles can increase their density after excess photosynthesis (Thomas and Walsby, 1985; Visser et al., 1995), hereby increasing their settling velocity. The settling velocity of phytoplankton is higher when it is combined to other suspended particles. Flocs, composed of extracellular polymer matter and diatoms have for instance been observed (Engel, 2000; Kiørboe et al., 1994, 1990). Flocs, made of diatoms and sediment particles have also been reported (Avnimelech et al., 1982; Søballe and Threlkeld, 1988). In our case, the the algae particles can indeed be observed in the whole water columnm, as chlorophyll concentrations (CC) could be measured at all depths, see Figure 7. As the dependence of chlorophyll concentrations (CC) is linear with suspended sediment concentration (SSC) it emables us to define a CC/SSC ratio. In section 4.2.1, we will study the relation between D50, shear rate and depth as function of the CC/SSC ratio. In section 4.2.2, we will detail laboratory experiments, to check hypothesis 1 and 3.

4.2.1 Algae-sediment ratio in in-situ conditions

From Figure 7 it can be inferred that the chlorophyll (CC) to sediment (SSC) ratio is larger for neap than spring tide, which implies that for a given SSC there will be more algae in the suspension

at neap (low shears) than at spring (high shears). This is in line with the results of section 4.1, where it was found that at neap the density of the particles in suspension is lower than at spring. This would agree with the fact that mineral-based aggregates are denser than algae-based aggregates: at spring, more mineral sediment can be transported in the water column, whereas at neap most of the mineral-based aggregates would be deposited and predominantly algae-based aggregates would remain in suspension.

The CC/SSC ratios are also different for different shear rates: the CC/SSC data is scattered at low shear rate, close to the top of the water column. In that part of the water column algae are dominant, and the sediment concentration is quite low. Considering the optical properties of algae, we raise the question whether the OBS can properly estimate the SSC concentrations in that part of the water column. As the water samples taken to be measured in the laboratory have been filtered, it is also possible that some biomass is lost in the process. This implies that the SSC correlation (in-situ/lab) shown in Figure 2 does not display significant outliners at low SSC. In the middle part of the water column, where higher shear rates (5–10 s^{-1}) and higher SSC are observed, the correlation between SSC and CC is significant, and the CC/SSC ratios are higher than at the bottom of the water column.

The high SSC concentration close to the bottom is a result of the erosion of the bed due to the high shear (> 10 s^{-1}) at that position. As the deeper part of the eroded bed barely contains algae, this is the reason for the CC saturation value (Xu et al., 2016). At neap, the SSC close to the bottom is much less than at spring tide, and only the upper layer (containing algae) of the bed is eroded, resulting in a better correlation between CC and SSC for any SSC.

The floc size as function of CC/SSC ratio is displayed in Figure 8. It is clear, from comparing

Figure 8a and Figure 8b that the data is quite scattered for the measurements done at low shear, for the particles found at the top of the water column, i.e. 0H and 0.2H. This could, as indicated at the beginning of this section, correspond to the fact that at the top of the water column mainly algae are present and that the CC/SSC ratio is ill defined. At higher depths (0.4H-1H) the ratio CC/SSC is rather constant, at a value in the range 2-4 $\mu g \cdot g^{-1}$ at spring and 2-5 $\mu g \cdot g^{-1}$ at neap, indicating that there is more algae in the water column at neap than at spring. For this CC/SSC ratio the D50 varies between 10-80 μm, the smallest D50 are found at high shear and the largest D50 at low shear, as expected.

Despite the the limited amount of data points, one can observe that the largest D50 are found for the highest CC/SSC in the range 1-5 $\mu g \cdot g^{-1}$. This is also the case for the data points above 5 $\mu g \cdot g^{-1}$, even though the data is very scattered as discussed above . We wanted to confirm this by laboratory experiments. This is done in the next section.

4.2.2 Algae-sediment flocculation process in laboratory

From the data collected in-situ, it was not possible to assess (1) whether the D50 increases with CC/SSC ratio , (2) whether the algae-sediment mixture can reach a monomodal steady-state (hypothesis 3) and if algae-algae flocculation and sediment-sediment flocculation would occur significantly over algae-sediment flocculation (hypothesis 1). To verify these points, laboratory experiments were performed.

The experiments were done using Yangtse sediment, collected in the sediment bed. Even though the sediment samples might contain some (degraded) algae, the bottom shear stresses at the sampling site ensure that the sediment is very well mixed and a low content in algae is expected

(Zhang et al., 2007; Zhu et al., 2011). This is also confirmed from the analysis of the in-situ data, where we have shown that small and dense particles are resuspended from the bed at high shear (section 4.1).

It was first verified that the Yangtse sediment, collected in the sediment bed, has a limited flocculation ability. An amount of 0.7 $g \cdot l^{-1}$ of this sediment, dispersed in artificial sea water was stirred (at 40 rpm, roughly equivalent to a shear rate of 90 s^{-1}) in 1L jar, and particle size distributions were recorded for 3 hours by static light scattering. The mean particle size varied from 8.6 μm to 11.2 μm within 10 min and then remained constant, see Figure 9a.

In a second series of tests, *Skeletonema costatum* was studied (Riper et al., 1979; Smayda and Boleyn, 1966). 5×10^5 cells were dispersed in artificial sea water in 1L jar, gently stirred (at 40 rpm), and particle size distributions were recorded for 5 hours by static light scattering. The mean particle size varied as indicated in Figure 9b.

The initial particle size distribution is in agreement with the shape of *Skeletonema costatum* as observed by microscope (Figure 10). A single *Skeletonema costatum* cell is about 4-6 μm wide. The *Skeletonema costatum* cultures produce distributions of single cells, but, by cell division or aggregation of cells with neighboring ones, 2 cell-long chains and sometimes 3, 4 or 5 cell-long chains can be observed. The chains length can reach lengths of 30 μm (Capriulo et al., 1988; Gibson et al., 1993; Nayar et al., 2005). In time, the cells flocculate or divide, creating particles of equivalent diameter of about 40–100 μm.

The aggregates observed under microscope were never longer than 50 μm because of the manipulation required to observe them by microsopy: longer aggregates are broken when the cover slip is slid over the sample.

In time, the mean particle size D50 (see insert in Figure 9) is significantly increasing, indicating that either the algae particles are flocculating, or their chains are growingThe larger peak of the distribution reaches a steady-state after 30 min. The concentration algae used in the laboratory experiments is comparable with the values obtained in-situ, as it was estimated that 4×10^4 cells·l^{-1} *Skeletonema costatum* corresponds to 1 μg·l^{-1} chlorophyll-a concentration in Yangtze estuary (Bulletin, 2014)., The estimated experimental chlorophyll-a concentration varies from 1.25 μg·l^{-1} to 12.5 μg·l^{-1}.

In the next series of tests, Yangtse sediment and *Skeletonema costatum* was mixed together and the time evolution of the PSD was recorded (Figure 11). From Figure 11a, it is clear that sediment-algae flocs can form rapidly when mixed, as the particle size curve shifts from bimodal to unimodal in 10 minutes. As the hydrodynamics in the jar are different from in-situ, the kinetics of aggregation might however be different in-situ. From Figure 11b, it can be observed that the ratio of sediment and algae concentration plays a dominant role in determining the equilibrium particle size. The red and blue curves correspond to the case where the CC/SSC ratio is the same (18 μg/g), but the algae and sediment concentrations are ten times higher for the red curve than the blue curve. The same D50 is obtained in this case. When the CC/SSC is lower (CC/SSC = 1.8 μg·g^{-1}, yellow curve compared to the red and blue curves CC/SSC = 18 μg·g^{-1}*)* the D50 is lower. It does not matter whether the CC/SSC (yellow curve) is lower because there are less algae but same amount of sediment (red curve) or more sediment and same amount of algae (blue curve) These results seem to indicate that when there is a relative abundance of algae compared to sediment particles, algae cells will aggregate with themselves to form large flocs (red and blue curves), but that when the sediment concentration is substantial in comparison with the algae concentration, the limiting factor

will be the sediment concentration (yellow curve). Due to the binding of algae with sediment, there are no algae left to form large algae-algae aggregates.

We have shown that in the laboratory (1) the D50 increases with CC/SSC ratio and (2) the algae-sediment mixture can reach a monomodal steady-state There is a significant algae-algae flocculation but no sediment-sediment flocculation.

4.2.3 Link between in-situ observations and lab measurements

In section 4.1, we have identified 3 classes of particles in-situ: (1) particles smaller than 5 μm (2) particles in the range 10-50 μm and (3) particles in the range larger than 100 μm. At the end of the same section, we have concluded that the particles smaller than 5 μm are mineral sediment particles, resuspended from the bed at high shears and large particles (> 100 μm) are algae, which are present at all depths and all times, their largest relative amount being at slack.

The in-situ and laboratory data are compared in Figure 12.

The peak in size of the mineral sediment taken from the bed and analysed in the laboratory matches the peak in size corresponding to the middle fraction at spring (around 10-50 μm). This is consistent with the fact that at high shears, larger and denser particles (mineral sediment) can be eroded from the bed.

In the lab experiments, due to technical limitation (to avoid that particles would deposit in the pipes and at the bottom of the jar), the shear rate (90 s^{-1}) always larger than the in-situ shear rate (<60 s^{-1}). For this reason, and also because the diameter of the tubes was 6 mm it was not possible to obtain the largest floc sizes (> 500 μm) observed in-situ. Nonetheless, see Figure 12, it can be observed

that the peak in size obtained for algae at steady-state (around 200-300 μm) is very close to the peak for the highest particle size > 100 μm that is present in-situ at all depths and all times. This would tend to prove that this large particles in-situ are flocculated algae particles that have reached an equilibrium size.

The broad peak in size observed at LWS, for both spring and neap, at the bottom the water column (0.6H-1H) lays in the range 50-200 μm and is in good agreement with the steady-state peak observed in the lab for CC/SSC = 1.8 $\mu g \cdot g^{-1}$. This CC/SSC is of the same order of magnitude than the CC/SSC ratio obtained in-situ (see Table 1). This would tend to prove that the particles corresponding to this in-situ peak are a mixture of algae and sediment. From the result found in 4.2.2 it is expected that for a lower CC/SSC ratio this peak in size would shift towards smaller sizes. This is indeed observed for the PSD's displayed in Figure 5, see also Table 1. The CC/SSC ratio at spring MFV and MEV is 1.2 and 1.5 $\mu g \cdot g^{-1}$, where the D50 is 17 and 23 μm, and it is 5.5 and 3.5 $\mu g \cdot g^{-1}$ at neap HWS and LWS where the D50 is 54 and 50 μm.

5. Conclusions

By combining the analysis of in-situ data and laboratory experiments, it was found that the presence of algae (the species *Skeletonema costatum* was used for laboratory experiments as being representative for the dominant species in-situ) plays a major role in explaining the particle size distributions, and in particular the multimodal distribution observed in the Yangtse estuary. Three particle classes have been defined, correponding to peaks in size observed in the Particle Size Distributions (PSD's): (1) particles smaller than 5 μm (2) particles in the range 10-50 μm and (3) particles in the range larger than 100 μm. The algae was found in the whole water column, for any

tidal condition, as Chlorophyll A concentration (a proxy for the algae concentration), CC, could be measured at any depth. The suspended sediment concentration (SSC) was linearly linked to the CC which led us to study the CC/SSC ratio as function of shear, particle size and position in the water column . The discussion in section 4 can be summarized in a conceptual figure (Figure 13), where we divide the suspended sediment into three types: (mineral) sediment dominated, sediment-algae and algae dominated. All three types are present in the Yangtse estuary.

In the absence of algae, sediment particles can flocculate due to the presence of salt but this flocculation will happen in the fresh to salt water transition region of the estuary. As demonstrated in the laboratory experiments, there will be no further flocculation of sediment flocs in saline water. The size of mineral sediment particles can be small (<5 μm) as found at maximum velocities (see Figure 5), but there can also be a significant amount of mineral sediment in larger flocs (10 μm peak in Spring-MEV, see Figure 12) at high shears.

The primary algae cells, on the other hand, can easily flocculate with themselves, also in saline conditions as demonstrated in the laboratory experiments and this type of flocculation occurs in-situ, leading to the presence of large (> 100 μm) flocs in the whole water column, at any hydrodynamic condition . The size of algae flocs (usually large) will depend on the algae species and the climate conditions. In the laboratory we demonstrated that the algae *Skeletonema costatum* has a dynamic particle size, as, in time, the algae cells flocculate or divide, creating larger particles. When mineral sediment and *Skeletonema costatum* are mixed together in the laboratory, the PSD changed rapidly from a bimodal PSD to a monomodal PSD. The D50 of this monomodal PSD (corresponding roughly to the in-situ middle peak size 10-50 μm which is also in good approximation equal to the in-situ D50) is a function of the algae to sediment CC/SSC ratio : the

D50 is larger for a larger CC/SSC. In fact, from the laboratory experiments, we found that the presence of sediment is the limiting growth factor. The algae flocs are largest in the absence of sediment, and the more sediment (relative to the concentration of algae), the smaller the flocs. -

In the Estuary Tubidity Maximum (ETM) Zone studied in the present article, depending on the tidal period, the shear stresses and the position in the water column, different particle size distributions were observed. These distributions ranged from small monomodal size peaks (sediment and single algae cells) to large monomodal size peaks (algae flocs), but with a predominance of monomodal and bimodal size peaks corresponding to sediment-algae flocs. Bimodal size distributions were also observed in the laboratory experiments for sediment-algae mixtures, but only at short times, as the optimized mixing of sediment and algae in the jar quickly led to a monomodal equilibrium particle size.

This leads us to conclude, in view of the hypothesis 1 and 3 given in the introduction, that in the ETM zone:

- there are two types of particles (sediment and algae), that most probably the large algae flocs (> 100 μm) have been formed in a region devoid of sediment particles and the lowest size fraction (< 5 μm) is composed of sediment particles eroded from the bed at high shears

- the PSD's are usually not fully at steady-state as the middle size fraction (10-50 μm) is shifting in size according to shear and position in the water column. This middle size fraction is composed of sediment and algae particles and their relative amount is depending on the hydrodynamic condition and position in the water column.

Regarding the modelling of sediment-algae suspensions in the Yangtse estuary, all three particle sizes should be accounted for. A key parameter for predicting the position of the middle size

peak is the CC/SSC ratio .

Acknowledgements

This research is the joint-program between SKLEC (State Key Lab of Estuarine and Coastal Research, China) and TU Delft (the Netherlands). The authors wish to thank Prof. Peter Herman and Dr. Thijs van Kessel for useful discussions. Deltares is gratefully acknowledged for the use of the laboratory equipment. Financial support was provided by the Natural Science Foundation of China (No. 51320105005, 51739005), Shanghai Science and Technology Committee (No.17DZ1204800) and State Scholarship Fund of The China Scholarship Council (No.201606140063).

Reference

Andrews, S., Nover, D., Schladow, S.G., 2010. Using laser diffraction data to obtain accurate particle size distributions: the role of particle composition: Laser diffraction data processing. Limnology and Oceanography: Methods 8, 507–526. https://doi.org/10.4319/lom.2010.8.507

Avnimelech, Y., Troeger, B.W., Reed, L.W., 1982. Mutual flocculation of algae and clay: evidence and implications. Science 216, 63–65. https://doi.org/10.1126/science.216.4541.63

Baker, E.., Tennant, D.., Feely, R.., Lebon, G.., Walker, S.., 2001. Field and laboratory studies on the effect of particle size and composition on optical backscattering measurements in hydrothermal plumes. Deep Sea Research Part I: Oceanographic Research Papers 48, 593–604. https://doi.org/10.1016/S0967-0637(00)00011-X

Baker, E.T., Lavelle, J.W., 1984. The effect of particle size on the light attenuation coefficient of natural suspensions. Journal of Geophysical Research 89, 8197. https://doi.org/10.1029/JC089iC05p08197

Barlow, J.P., 1955. Physical and Biological Processes Determining the Distribution of Zooplankton in a Tidal Estuary. The Biological Bulletin 109, 211–225. https://doi.org/10.2307/1538722

Bouyer, D., Liné, A., Do- Quang, Z., 2004. Experimental analysis of floc size distribution under different hydrodynamics in a mixing tank. AIChE Journal 50, 2064–2081. https://doi.org/10.1002/aic.10242

Bulletin, 2014. China Inshore Waters Environment Quality Bulletin.

Camp, T.R., 1943. Velocity gradients and internal work in fluid motion. J. Boston Soc. Civ. Eng. 30,

219–230.

Capriulo, G.M., Schreiner, R.A., Dexter, B.L., 1988. Differential growth of Euplotes vannus fed fragmented versus unfragmented chains of Skeletonema costatum. Marine Ecology Progress Series 205–209. https://doi.org/10.3354/meps047205

Chassagne, C., Mietta, F., Winterwerp, J.C., 2009. Electrokinetic study of kaolinite suspensions. Journal of Colloid and Interface Science 336, 352–359. https://doi.org/10.1016/j.jcis.2009.02.052

Chen, J., 1995. Sediment dynamics and evolution of the mouthbar and subaqueous delta in the Yangtze estuary. Pesources & Enuironment in the Yangtza Valley.

Chen, M.S., Wartel, S., Temmerman, S., 2005. Seasonal variation of floc characteristics on tidal flats, the Scheldt estuary. Hydrobiologia 540, 181–195. https://doi.org/10.1007/s10750-004-7143-6

Chen, S., Eisma, D., 1995. Fractal geometry of in situ flocs in the estuarine and coastal environments. Netherlands Journal of Sea Research 33, 173–182. https://doi.org/10.1016/0077-7579(95)90004-7

Cheng, J., 2004. The characteristic of suspended fine sediment flocs in Changjiang estuary (Master Thesis). East China Normal University.

Chien, N., Wan, Z., 1999. Mechanics of Sediment Transport. American Society of Civil Engineers, Reston, VA. https://doi.org/10.1061/9780784404003

de Lucas Pardo, M., 2014. Effect of biota on fine sediment transport processes: A study of Lake Markermeer (Ph. D. Thesis). TU Delft, Delft University of Technology.

Dontsova, K.M., Bigham, J.M., 2005. Anionic Polysaccharide Sorption by Clay Minerals. Soil Science Society of America Journal 69, 1026. https://doi.org/10.2136/sssaj2004.0203

Droppo, I.G., 2001. Rethinking what constitutes suspended sediment. Hydrological Processes 15, 1551–1564. https://doi.org/10.1002/hyp.228

Eisma, D., 1986. Flocculation and de-flocculation of suspended matter in estuaries. Netherlands Journal of Sea Research 20, 183–199. https://doi.org/10.1016/0077-7579(86)90041-4

Eisma, D., Li, A., 1993. Changes in suspended-matter floc size during the tidal cycle in the dollard estuary. Netherlands Journal of Sea Research 31, 107–117. https://doi.org/10.1016/0077-7579(93)90001-9

Engel, A., 2000. The role of transparent exopolymer particles (TEP) in the increase in apparent particle stickiness (α) during the decline of a diatom bloom. Journal of Plankton Research 22, 485–497. https://doi.org/10.1093/plankt/22.3.485

Fennessy, M.J., Dyer, K.R., 1996. Floc population characteristics measured with INSSEV during the Elbe estuary intercalibration experiment. Journal of Sea Research 36, 55–62. https://doi.org/10.1016/S1385-1101(96)90771-6

Fettweis, M., 2008. Uncertainty of excess density and settling velocity of mud flocs derived from in situ measurements. Estuarine, Coastal and Shelf Science 78, 426–436. https://doi.org/10.1016/j.ecss.2008.01.007

Fettweis, M., Baeye, M., Van der Zande, D., Van den Eynde, D., Joon Lee, B., 2014. Seasonality of floc strength in the southern North Sea. Journal of Geophysical Research: Oceans 119, 1911–1926. https://doi.org/10.1002/2013JC009750

Fettweis, M., Lee, B.J., 2017. Spatial and Seasonal Variation of Biomineral Suspended Particulate Matter Properties in High-Turbid Nearshore and Low-Turbid Offshore Zones. Water 9, 694.

https://doi.org/10.3390/w9090694

Filippa, L., Freire, L., Trento, A., Álvarez, A.M., Gallo, M., Vinzón, S., 2011. Laboratory evaluation of two LISST-25X using river sediments. Sedimentary Geology 238, 268–276. https://doi.org/10.1016/j.sedgeo.2011.04.017

Gibson, C.E., McCall, R.D., Dymond, A., 1993. Skeletonema subsalsum in a freshwater irish lake. Diatom Research 8, 65–71. https://doi.org/10.1080/0269249X.1993.9705239

Guan, X., Chen, Y., 1995. Experimental study on dynamic formula of sand coagulation sinking in stationary water in Changjiang estuary. Ocean Engineering.

Guan, X., Chen, Y., Du, X., 1996. Experimental study on mechanism of flocculation in Yangtze estuary. Journal of Hydraulic Engineering.

Guo, C., He, Q., Guo, L., Winterwerp, J.C., 2017. A study of in-situ sediment flocculation in the turbidity maxima of the Yangtze Estuary. Estuarine, Coastal and Shelf Science 191, 1–9. https://doi.org/10.1016/j.ecss.2017.04.001

He, Q., Sun, J., 2009. The Netz-phytoplankton community in Changjiang(Yangtze) River Estuary and adjacent waters. Acta ecologica sinica/Shengtai Xuebao 29.

Huiming, Z., Hongwei, F., Minghong, C., 2011. Floc architecture of bioflocculation sediment by ESEM and CLSM. Scanning 33, 437–445. https://doi.org/10.1002/sca.20247

Jiang, Z., Liu, J., Chen, J., Chen, Q., Yan, X., Xuan, J., Zeng, J., 2014. Responses of summer phytoplankton community to drastic environmental changes in the Changjiang (Yangtze River) estuary during the past 50 years. Water Research 54, 1–11. https://doi.org/10.1016/j.watres.2014.01.032

Kiørboe, T., Andersen, K.P., Dam, H.G., 1990. Coagulation efficiency and aggregate formation in marine phytoplankton. Marine Biology 107, 235–245. https://doi.org/10.1007/BF01319822

Kiørboe, T., Lundsgaard, C., Olesen, M., Hansen, J.L., 1994. Aggregation and sedimentation processes during a spring phytoplankton bloom: A field experiment to test coagulation theory. Journal of Marine Research 52, 297–323. https://doi.org/10.1357/0022240943077145

Knap, A., Michaels, A., Close, A., Ducklow, H., Dickson, A., 1996. Protocols for the joint global ocean flux study (JGOFS) core measurements.

Law, B.., Milligan, T.G., Hill, P.S., Newgard, J., Wheatcroft, R.A., Wiberg, P.L., 2013. Flocculation on a muddy intertidal flat in Willapa Bay, Washington, Part I: A regional survey of the grain size of surficial sediments. Continental Shelf Research 60, S136–S144. https://doi.org/10.1016/j.csr.2012.06.007

Lee, W.T.B.V.D., 2000a. Parameters affecting mud floc size on a seasonal time scale: The impact of a phytoplankton bloom in the Dollard estuary, The Netherlands. Proceedings in Marine Science 3, 403–421. https://doi.org/10.1016/S1568-2692(00)80134-5

Lee, W.T.B.V.D., 2000b. Temporal variation of floc size and settling velocity in the Dollard estuary. Continental Shelf Research 20, 1495–1511.

Liu, H., He, Q., Meng, Y., Wang, Y., Tang, J., 2007. Characteristics of surface sediment distribution and its hydrodynamic responses in the Yangtze River estuary. ACTA GEOGRAPHICA SINICA-CHINESE EDITION- 62, 81.

Maggi, F., 2013. The settling velocity of mineral, biomineral, and biological particles and aggregates in water. Journal of Geophysical Research: Oceans 118, 2118–2132.

https://doi.org/10.1002/jgrc.20086

Maggi, F., 2009. Biological flocculation of suspended particles in nutrient-rich aqueous ecosystems. Journal of Hydrology 376, 116–125. https://doi.org/10.1016/j.jhydrol.2009.07.040

Manning, A.J., 2010. Video Observations of Flocculated Sediment from Three Contrastingly Different Natural Environments in the USA, in: PiE 2010 Particles in Europe Villefranche-Sur-Mer, France 14-17 November 2010. p. 44.

Manning, A.J., Dyer, K.R., 1999. A laboratory examination of floc characteristics with regard to turbulent shearing. Marine Geology 160, 147–170. https://doi.org/10.1016/S0025-3227(99)00013-4

Manning, A.J., Schoellhamer, D.H., 2013. Factors controlling floc settling velocity along a longitudinal estuarine transect. Marine Geology 345, 266–280. https://doi.org/10.1016/j.margeo.2013.06.018

Mietta, F., 2010. Evolution of the floc size distribution of cohesive sediments. TU Delft, Delft University of Technology.

Mietta, F., Chassagne, C., Verney, R., Winterwerp, J.C., 2010. On the behavior of mud floc size distribution: model calibration and model behavior. Ocean Dynamics 61, 257–271. https://doi.org/10.1007/s10236-010-0330-2

Mikkelsen, O., Pejrup, M., 2001. The use of a LISST-100 laser particle sizer for in-situ estimates of floc size, density and settling velocity. Geo-Marine Letters 20, 187–195. https://doi.org/10.1007/s003670100064

Nayar, S., Goh, B.P.L., Chou, L.M., 2005. Dynamics in the size structure of Skeletonema costatum (Greville) Cleve under conditions of reduced photosynthetically available radiation in a dredged tropical estuary. Journal of Experimental Marine Biology and Ecology 318, 163–182. https://doi.org/10.1016/j.jembe.2004.12.013

Nopens, I., 2005. Modelling the activated sludge flocculation process: a population balance approach. PhDThesis, Ghent University, Belgium.

Passow, U., Alldredge, A.L., Logan, B.E., 1994. The role of particulate carbohydrate exudates in the flocculation of diatom blooms. Deep Sea Research Part I: Oceanographic Research Papers 41, 335–357. https://doi.org/10.1016/0967-0637(94)90007-8

Pejrup, M., Mikkelsen, O.A., 2010. Factors controlling the field settling velocity of cohesive sediment in estuaries. Estuarine, Coastal and Shelf Science 87, 177–185. https://doi.org/10.1016/j.ecss.2009.09.028

Plude, J.L., Parker, D.L., Schommer, O.J., Timmerman, R.J., Hagstrom, S.A., Joers, J.M., Hnasko, R., 1991. Chemical Characterization of Polysaccharide from the Slime Layer of the Cyanobacterium Microcystis flos-aquae C3-40. Appl Environ Microbiol 57, 1696–1700.

Pottsmith, C., 2015. LISST-100X Users Manual.

Riper, D.M., Owens, T.G., Falkowski, P.G., 1979. Chlorophyll Turnover in Skeletonema costatum, a Marine Plankton Diatom. PLANT PHYSIOLOGY 64, 49–54. https://doi.org/10.1104/pp.64.1.49

Smayda, T.J., Boleyn, B.J., 1966. Experimental observations on the flotation of marine diatoms. II. Skeletonema costatum and Rhizosolenia setigera: flotation of marine diatoms. Limnology and Oceanography 11, 18–34. https://doi.org/10.4319/lo.1966.11.1.0018

Søballe, D.M., Threlkeld, S.T., 1988. Algal-clay flocculation in turbid waters: Variations due to algal and mineral differences: With 4 figures in the text. SIL Proceedings, 1922-2010 23,

750–754. https://doi.org/10.1080/03680770.1987.11899705

Sutherland, T.F., Lane, P.M., Amos, C.L., Downing, J., 2000. The calibration of optical backscatter sensors for suspended sediment of varying darkness levels. Marine Geology 162, 587–597.

Thomas, R.H., Walsby, A.E., 1985. Buoyancy Regulation in a Strain of Microcystis. Microbiology 131, 799–809. https://doi.org/10.1099/00221287-131-4-799

van Leussen, W., 1999. The variability of settling velocities of suspended fine-grained sediment in the Ems estuary. Journal of Sea Research 41, 109–118. https://doi.org/10.1016/S1385-1101(98)00046-X

van Leussen, W., 1994. Estuarine Macroflocs and Their Role in Fine-Grained Sediment Transport (Ph. D. Thesis). University of Utrecht.

Verney, R., Lafite, R., Brun-Cottan, J.-C., 2009. Flocculation Potential of Estuarine Particles: The Importance of Environmental Factors and of the Spatial and Seasonal Variability of Suspended Particulate Matter. Estuaries and Coasts 32, 678–693. https://doi.org/10.1007/s12237-009-9160-1

Verney, R., Lafite, R., Claude Brun-Cottan, J., Le Hir, P., 2011. Behaviour of a floc population during a tidal cycle: Laboratory experiments and numerical modelling. Continental Shelf Research 31, S64–S83. https://doi.org/10.1016/j.csr.2010.02.005

Visser, P.M., Ibelings, B.W., Mur, L.R., 1995. Autunmal sedimentation of *Microcystis* spp. as result of an increase in carbohydrate ballast at reduced temperature. Journal of Plankton Research 17, 919–933. https://doi.org/10.1093/plankt/17.5.919

Walsby, A.E., 1968. Mucilage secretion and the movements of blue-green algae. Protoplasma 65, 223–238. https://doi.org/10.1007/BF01666380

Wang, Ying, Jiang, H., Jin, J., Zhang, X., Lu, X., Wang, Yueqi, 2015. Spatial-Temporal Variations of Chlorophyll-a in the Adjacent Sea Area of the Yangtze River Estuary Influenced by Yangtze River Discharge. International Journal of Environmental Research and Public Health 12, 5420–5438. https://doi.org/10.3390/ijerph120505420

Winterwerp, J.C., 2002. On the flocculation and settling velocity of estuarine mud. Continental Shelf Research 22, 1339–1360. https://doi.org/10.1016/S0278-4343(02)00010-9

Winterwerp, J.C., 1999. On the dynamics of high-concentrated mud suspensions (Ph. D. Thesis). TU Delft, Delft University of Technology.

Winterwerp, J.C., 1998. A simple model for turbulence induced flocculation of cohesive sediment. Journal of Hydraulic Research 36, 309–326. https://doi.org/10.1080/00221689809498621

Xu, Y., Li, X., Wang, H., Zhang, B., 2016. Characteristics of a macrozoobenthic community in the sea adjacent to the Yangtze River estuary during the wet season. Biodiversity Science 24, 811–819. https://doi.org/10.17520/biods.2016039

Zhang, J., Wu, Y., Jennerjahn, T.C., Ittekkot, V., He, Q., 2007. Distribution of organic matter in the Changjiang (Yangtze River) Estuary and their stable carbon and nitrogen isotopic ratios: Implications for source discrimination and sedimentary dynamics. Marine Chemistry 106, 111–126. https://doi.org/10.1016/j.marchem.2007.02.003

Zhu, Z.-Y., Ng, W.-M., Liu, S.-M., Zhang, J., Chen, J.-C., Wu, Y., 2009. Estuarine phytoplankton dynamics and shift of limiting factors: A study in the Changjiang (Yangtze River) Estuary and adjacent area. Estuarine, Coastal and Shelf Science 84, 393–401. https://doi.org/10.1016/j.ecss.2009.07.005

Zhu, Z.-Y., Zhang, J., Wu, Y., Zhang, Y.-Y., Lin, J., Liu, S.-M., 2011. Hypoxia off the Changjiang

(Yangtze River) Estuary: Oxygen depletion and organic matter decomposition. Marine Chemistry 125, 108–116. https://doi.org/10.1016/j.marchem.2011.03.005

Figures:

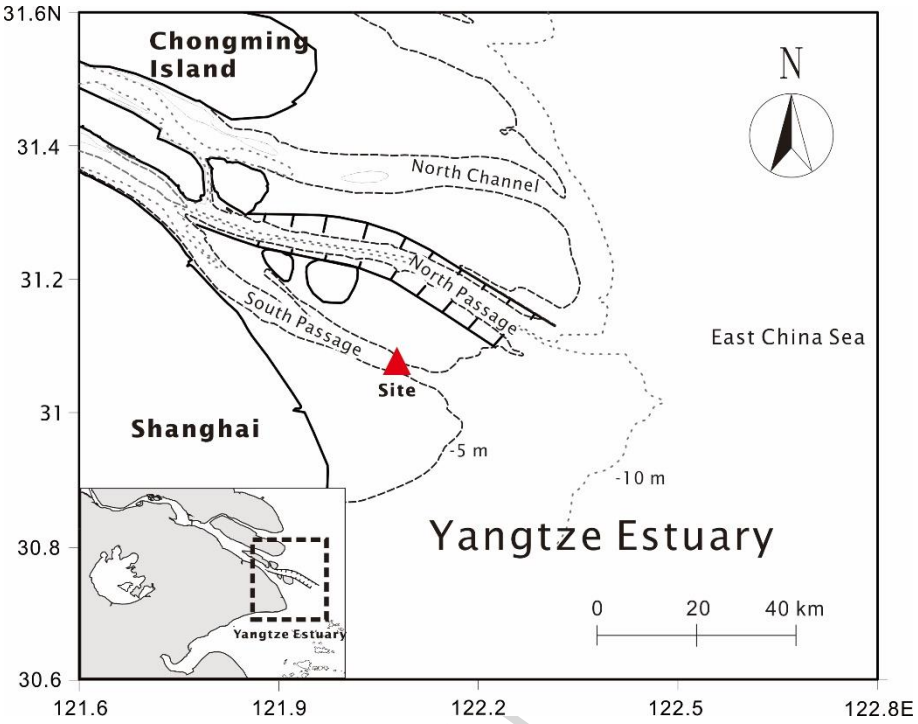

Figure 1 Study area of Yangtze Estuary. The local water depth of the study site (red star) is 5–9 m at spring tide and 5.3–8.3 m at neap tide.

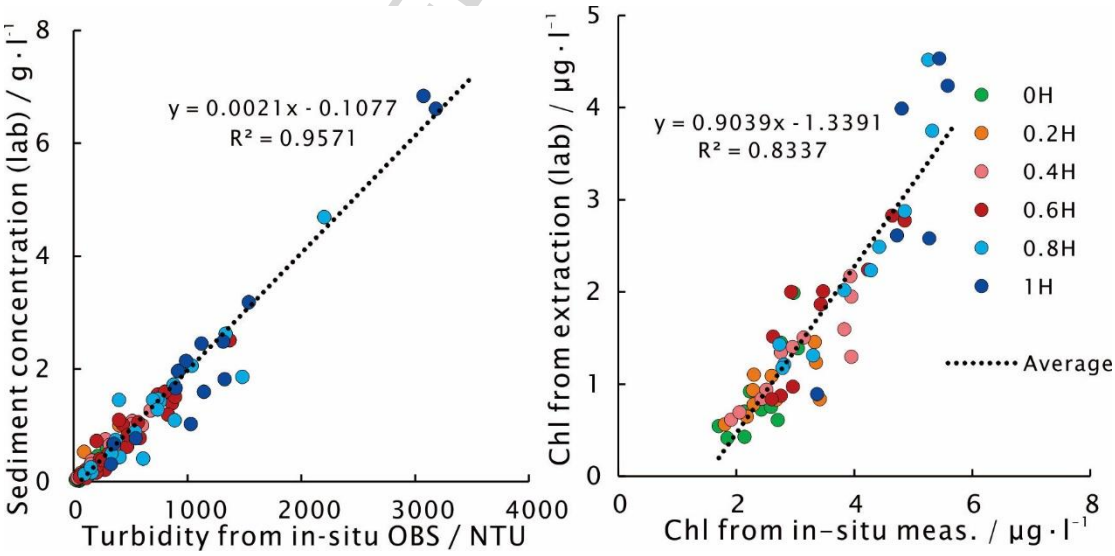

Figure 2 Calibration of the OBS (left) and Manta2 (right). Analysis from the water samples in the laboratory are compared to in-situ measurements. Linear fits between turbidities and chlorophyll-a concentrations gave a coefficient of determination (R^2) larger than 0.8 in both case. The depth in the water column is represented by the H position, where 0H represents the surface and 1H the bottom.

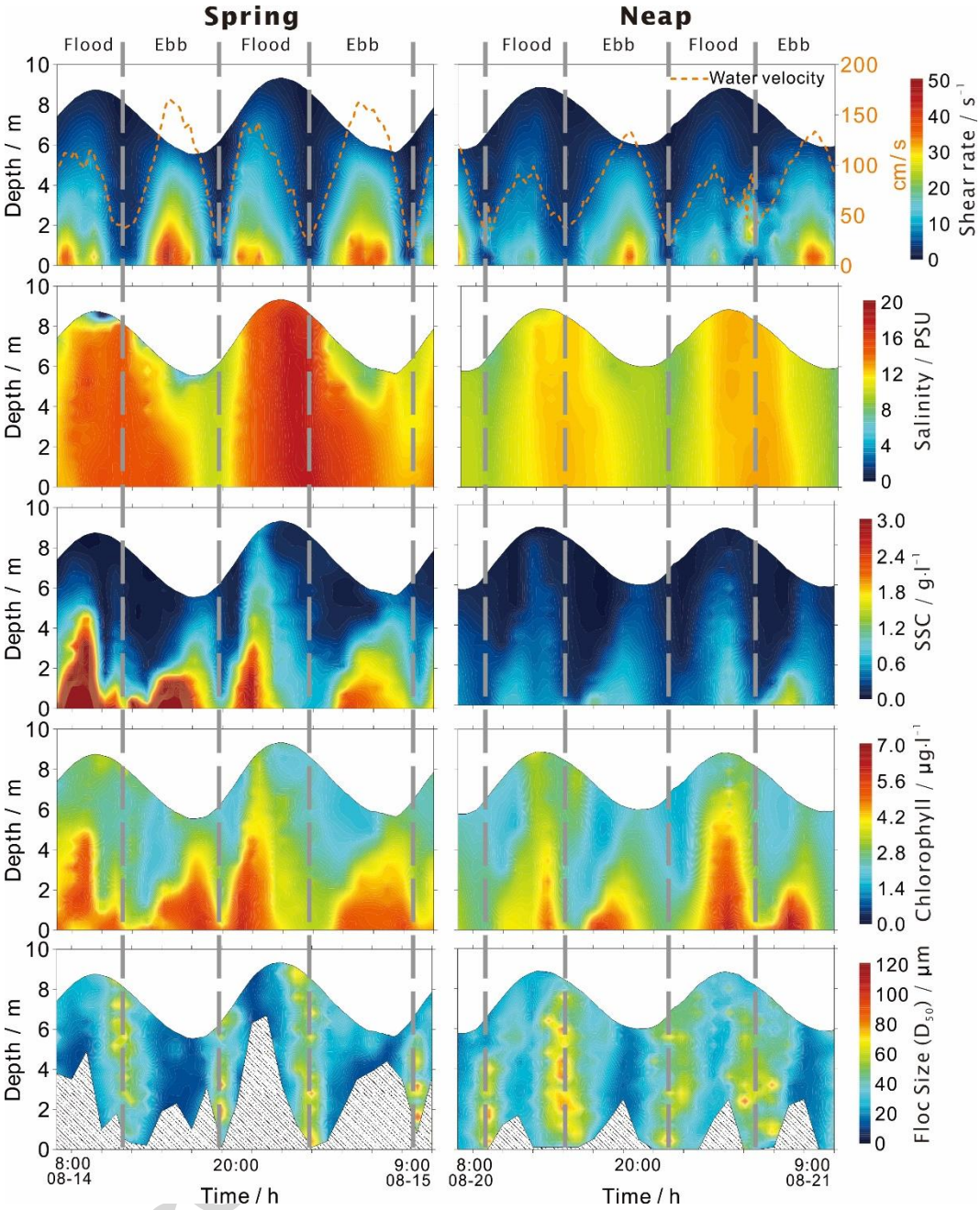

Figure 3 Distribution of shear stress, salinity, sediment concentration, chlorophyll-a concentration and mean floc size at spring tide.

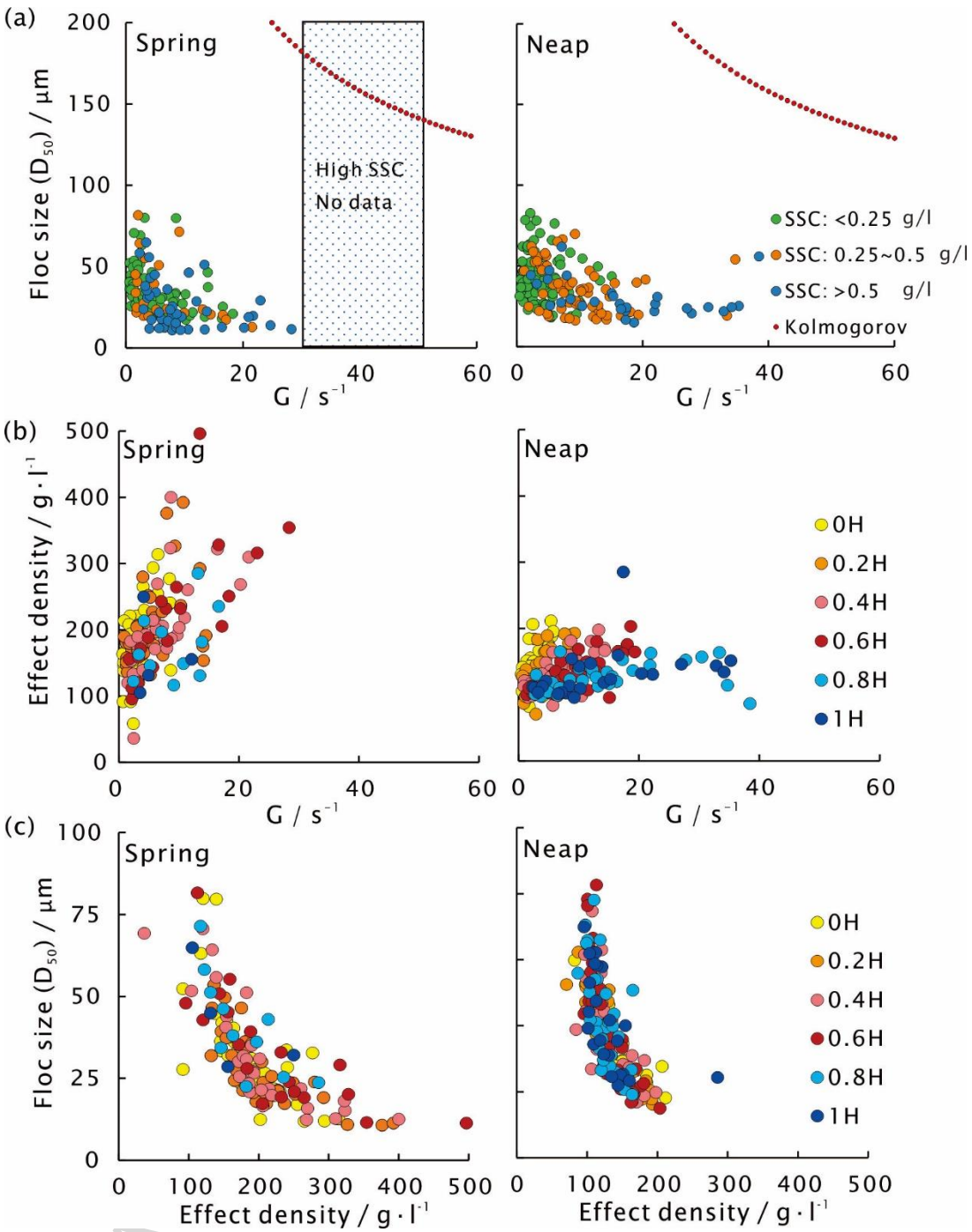

Figure 4 (a) D_{50} as function of shear for three SSC ranges; (b) density as function of shear for different depths and (c) D50 as function of effective densityfor different depths

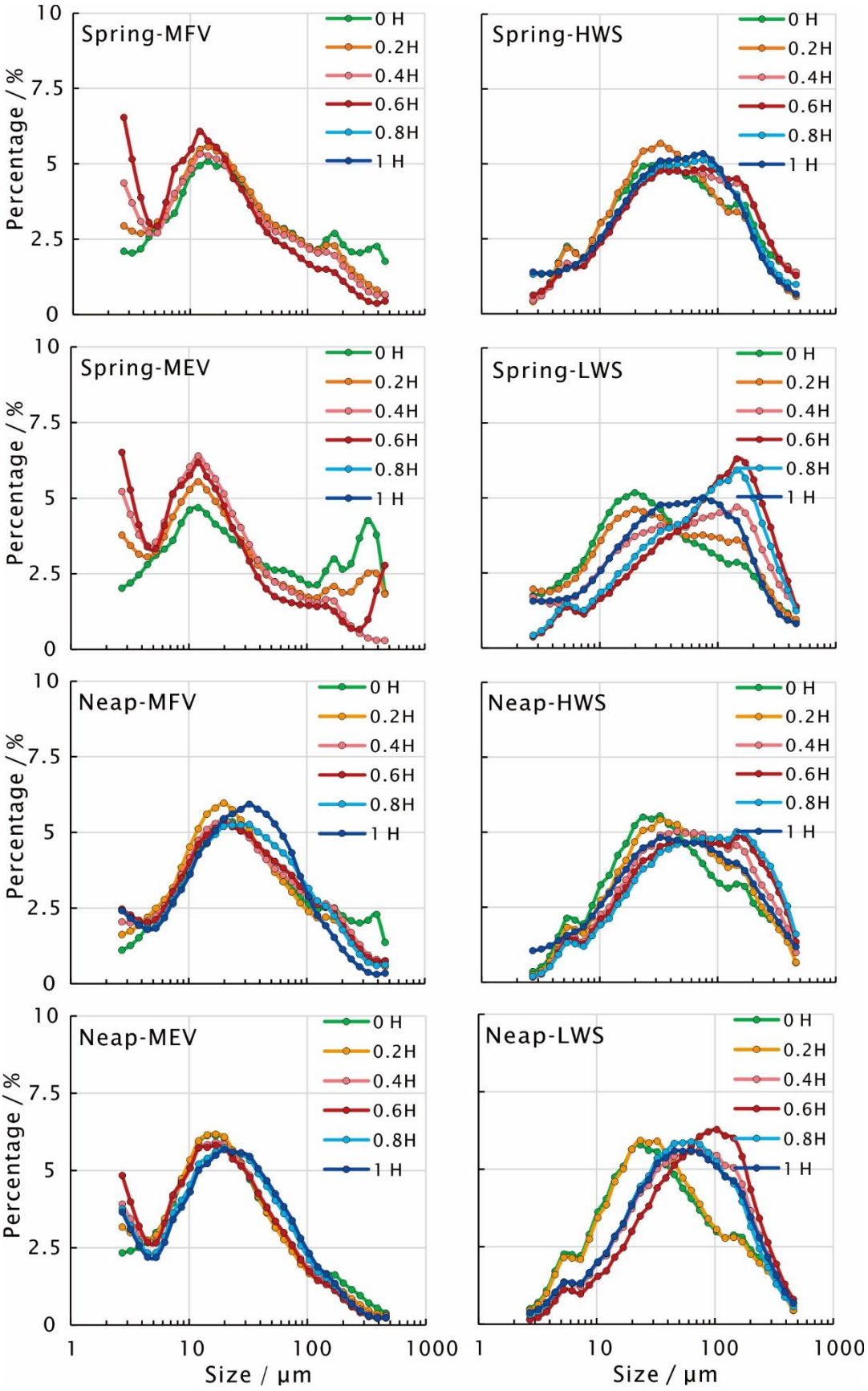

Figure 5 Particle size distributions at different tidal periods.

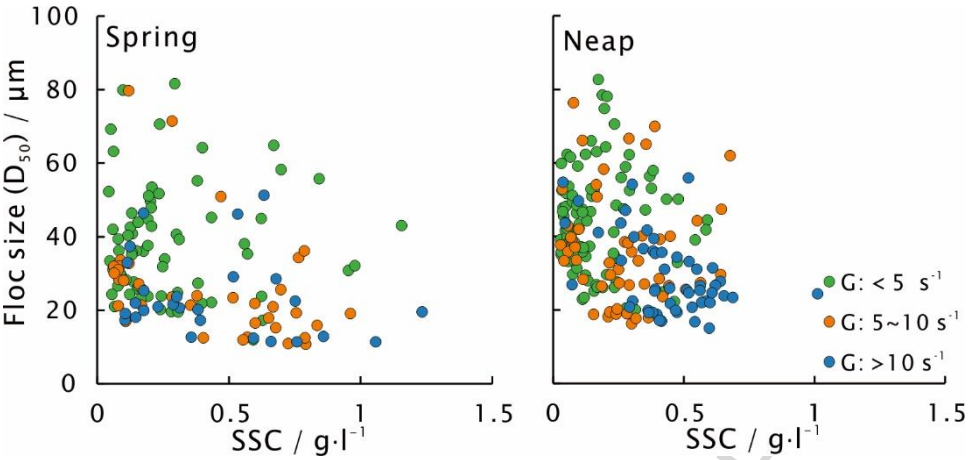

Figure 6 Variation of D_{50} with SSC for different shears

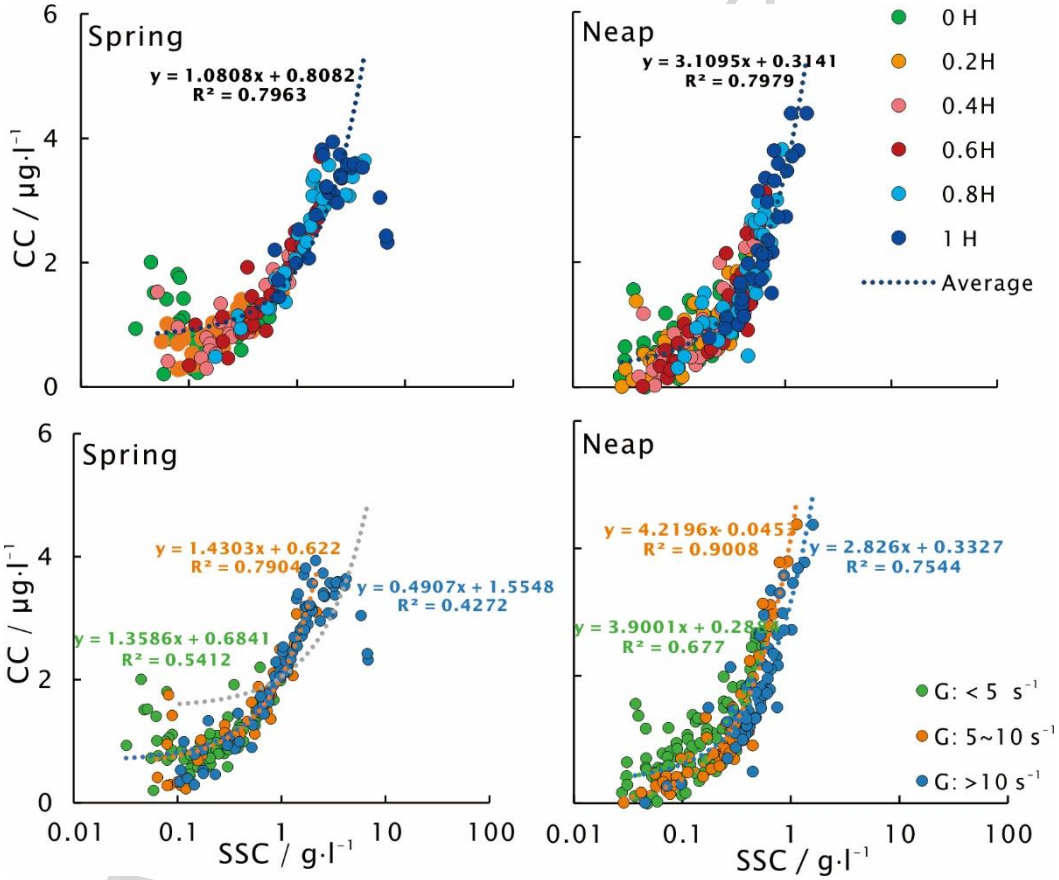

Figure 7 Relationship between chlorophyll-a concentration (CC) and sediment concentration (SSC)for different shears

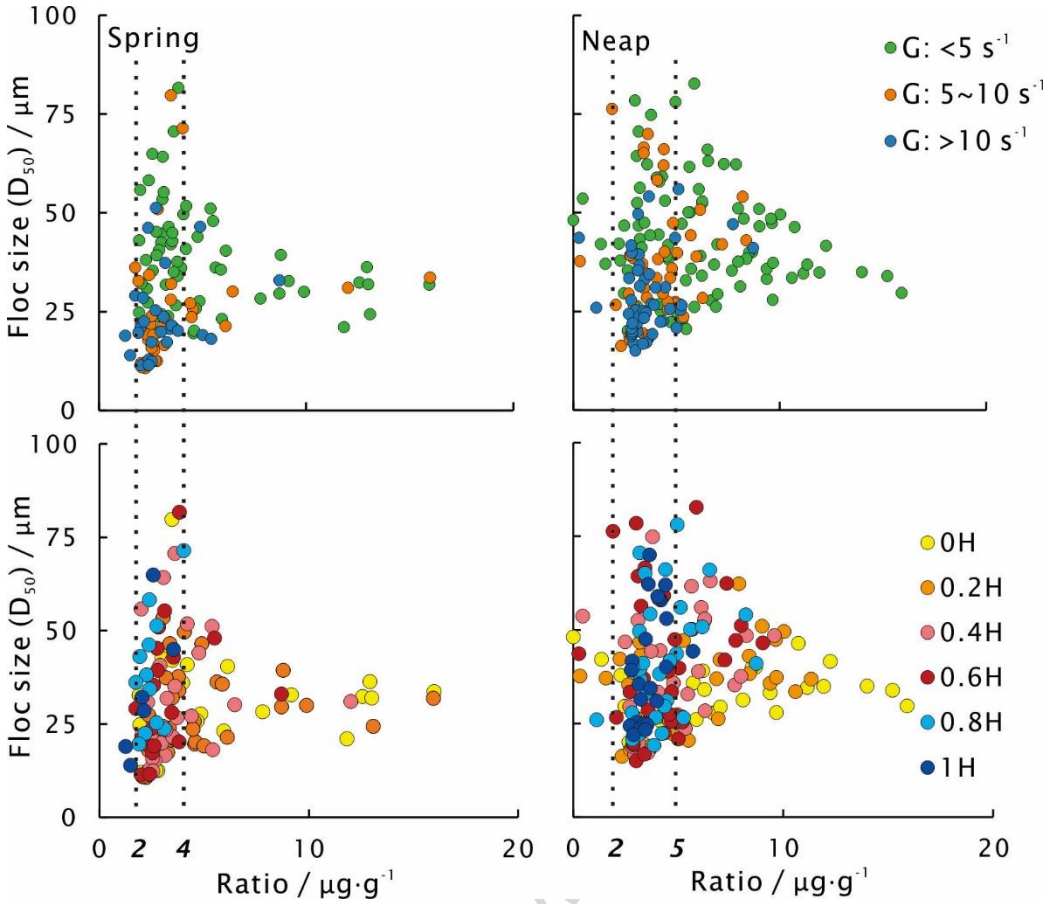

Figure 8 Relationship between floc size and CC/SSC ratio for different shears and different

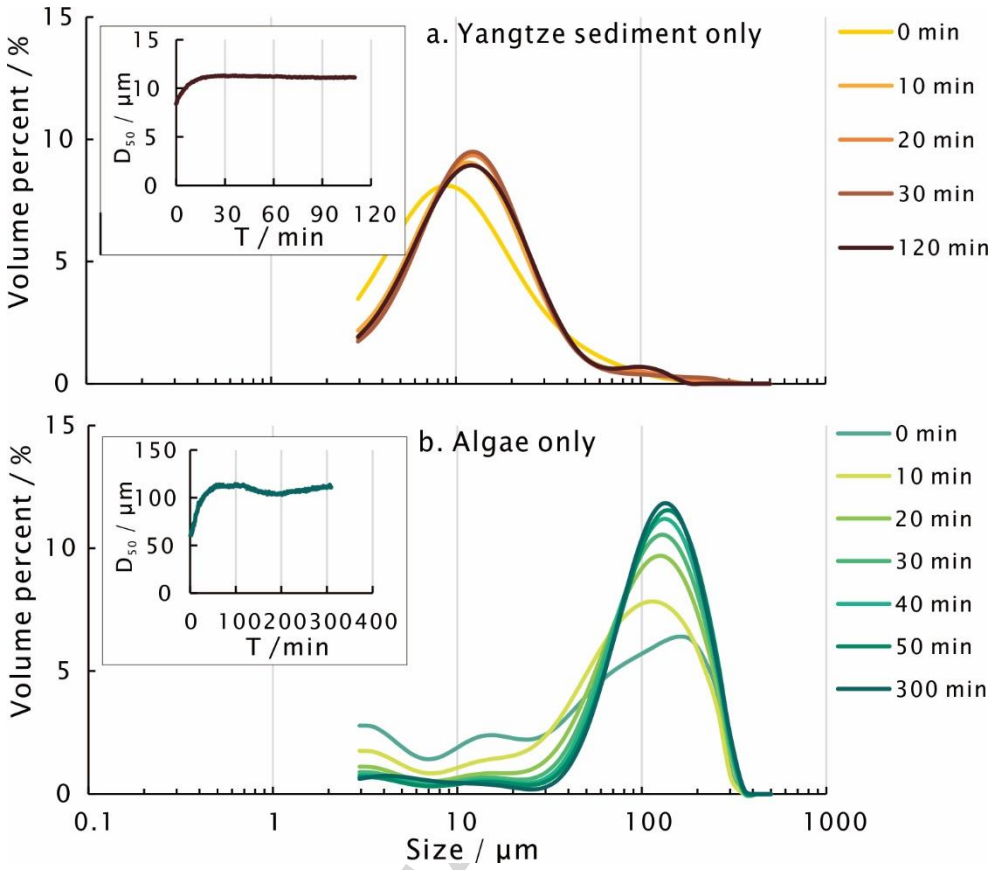

depths

Figure 9 Particle size distributions as function of time in artificial sea water, measured by static light scattering in the laboratory. (a): 0.7 g·l^{-1} of Yangtse sediment and (b) 5 × 10^5 cells·l^{-1} of Skeletonema costatum

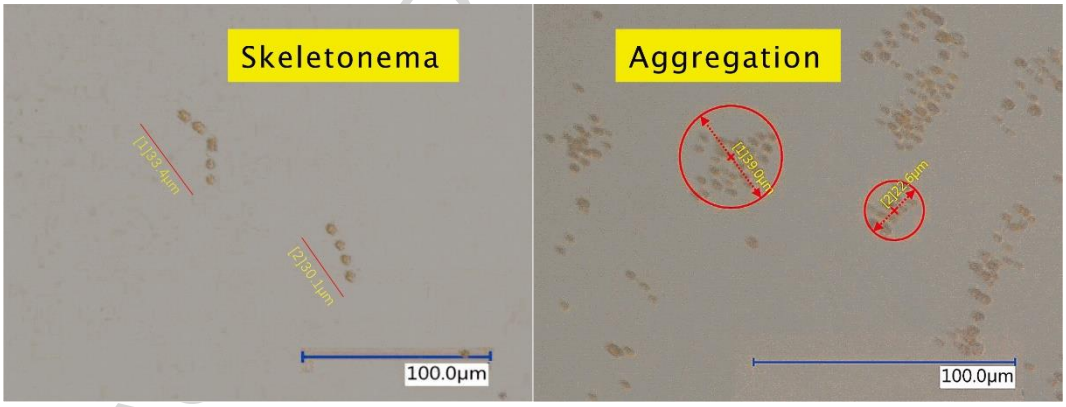

Figure 10 Skeletonema costatum and their aggregation

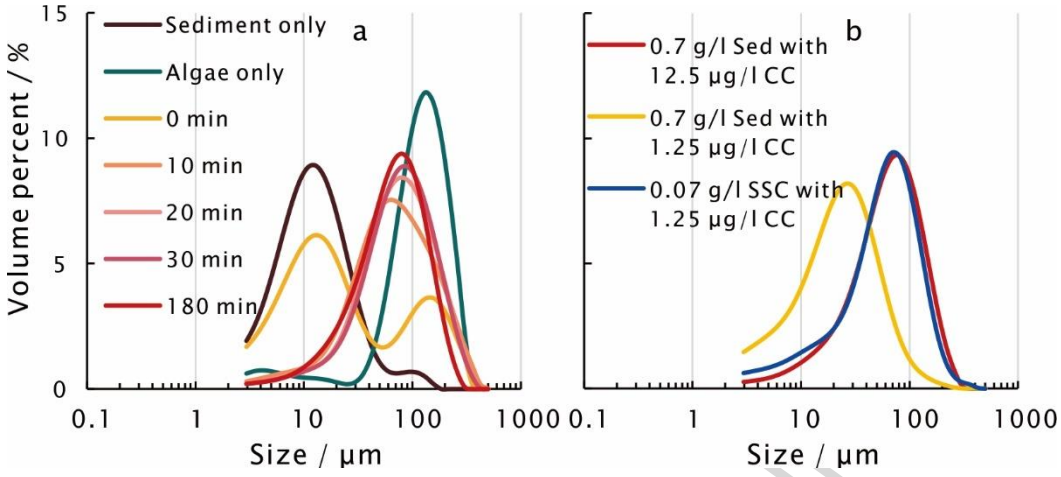

Figure 11 Aggregates of Yangtse sediment and Skeletonema costatum. (a) The PSD evolution of mixtures of sediment and algae. The time t=0 corresponds to the moment sediment and algae particles are mixed. The concentration of sediment was 0.7 g·l^{-1} and the concentration of algae was 5 × 10^{4}·l^{-1} cells (1.25 µg·l^{-1} CC) (b) Depending on the sediment to algae ratio, different equilibrium PSD are obtained.

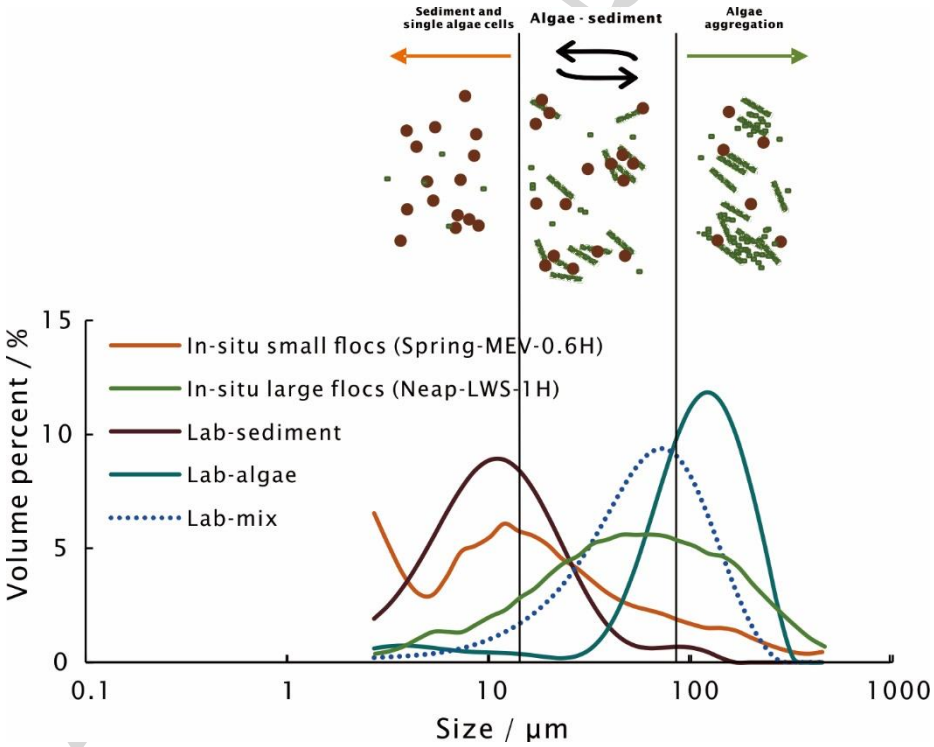

Figure 12 Comparison between in-situ and laboratory particle size distributions

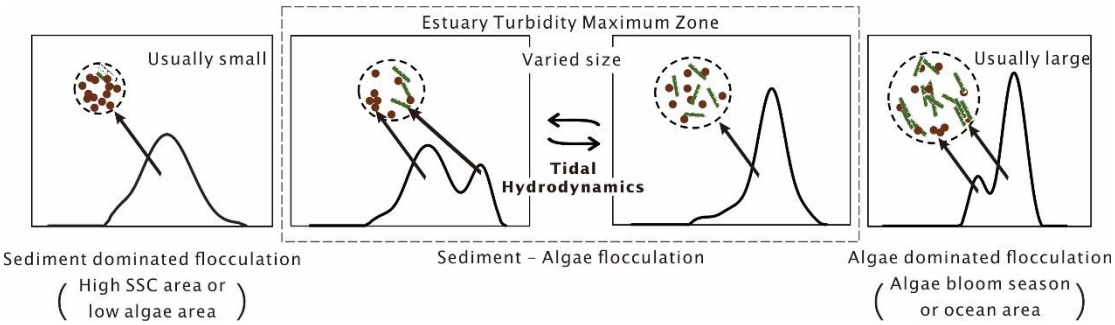

Figure 13 Schematic representation of algae-sediment flocculation in the Yangtse estuary.

Tables:

Table 1 *Mean water velocity, shear rate G, salinity Sal, suspended sediment concentration SSC, Chlorophyl-a concentration CC and particle size D_{50}, averaged over the whole water column*

		Velocity ($m \cdot s^{-1}$)	G (s^{-1})	Sal (PSU)	SSC ($g \cdot l^{-1}$)	CC ($\mu g \cdot l^{-1}$)	D_{50} (μm)
Spring tide	MFV	1.2	14.5	13.8	1.8	2.3	17.1
	HWS	0.4	2.4	15.9	0.6	1.4	45.3
	MEV	1.5	17.6	12.7	0.7	1.1	23.4
	LWS	0.4	3.5	10.8	0.7	1.8	48.8
Neap tide	MFV	1.0	10.6	12.1	0.4	2.0	26.8
	HWS	0.4	3.2	12.5	0.2	1.1	54.1
	MEV	1.3	18.2	9.8	0.5	1.4	18.9
	LWS	0.4	5.1	8.7	0.2	0.7	50.7

Highlights

•Shear rate plays a major role in floc size at all times and floc size decreasing with shear rate increasing.

• Algae play a major role in particle size distribution and could flocculate with sediment flocs in a different way in different shear condition.

• The ratio of sediment and algae is the key parameter that influences algae-sediment flocculation particle size distribution.